Inhibitory Effects of *Senna auriculata* Flower Extract-Prepared ZnO Pluronic F127 Sodium Alginate Nanoparticles Against Human Breast Cancer Cell Line (MDA-MB-237)

1*. Senthilkumar. G

2. Sakthivelu. A

1*. Research Scholar, PG and Research Department of Physics, Thanthai Periyar Government Arts and Science College (Autonomous), Tiruchirappalli – 620 023.Affiliated to Bharathidasan university, Tiruchirappalli,Tamilnadu, India. alpiry@gmail.com

2. Assistant Professor, PG and Research Department of Physics, Thanthai Periyar Government Arts and Science College (Autonomous), Tiruchirappalli – 620 023. Affiliated to Bharathidasan university, Tiruchirappalli,Tamilnadu, India.

Abstract

This investigation was carried out with the intention of expanding our knowledge of ZnO Pluronic F127 sodium alginate. ZnO Pluronic F127 sodium alginate NPs were subjected to X-ray diffraction analysis, which confirmed that they possess a wurtzite hexagonal structure. ZnO nanoparticles have recognisable peaks in their spectra at 446 cm^{-1}, and their FTIR spectra display the sodium alginate functional group as well as the Pluronic F127 overtone bands. In order to determine the morphologies of ZnO Pluronic F127 sodium alginate, a SEM examination was performed on the substance. Both the hydrodynamic sizes and the DLS spectra of ZnO Pluronic F127 chitosan nanoparticles are 181 nanometers. A blue emission peak can be seen at 478 nm in the PL spectra of ZnO Pluronic F127 sodium alginate NPs. This peak is caused by oxygen vacancies as well as other defects. The well-diffusion method was used to reevaluate the effectiveness of ZnO Pluronic F127 sodium alginate NPs and Amoxicillin against *Staphylococcus aureus, Klebsiella pneumoniae, Shigella dysenteriae, Bacillus*, and *Proteus valgaris*. A well diffusion apparatus was utilised in order to assess the degree to which nanoparticles were successful in obstructing the development of *Candida albicans*. When used to treat a human breast cancer cell line (MDA-MB-237), ZnO Pluronic F127 sodium alginate NPs displayed an anticancer activity that was comparable to that of the

control. The findings of this study lend credence to the hypothesis that ZnO nanoparticles that have been modified with biopolymers such as sodium alginate and copolymer pluronic F127 could find use in the manufacture of medical products.

Keywords: Pluronic F127 Sodium Alginate; ZnO; Breast cancer cell line; Antibacterial and Antifungal Activity; Anticancer activity;

*Corresponding author: alpiry@gmail.com

Introduction

The method to synthesise ZnO Nano size materials is one of the obstacles to attaining a standard anticancer therapy. Breast cancer incidence has climbed by over 20% since 2008 estimates, and mortality has increased by 14%, according to the latest global cancer statistics from the International Agency for research on cancer, WHO. Furthermore, in 120 of 184 countries, breast cancer is the most commonly diagnosed cancer in women. In 2012, it was responsible for 522,000 deaths among women. Presently, it accounts for over 25% of all cancer diagnoses in females. Lung cancer accounted for 1.6 million deaths (19.4 percent of all cancer deaths) according to the data. The early identification, diagnosis, and treatment of these lethal diseases is an essential need in cancer management today. New, effective, and cost-efficient methods are needed. Some common tumours may now be better treated using nano-medicine than in the past. This has led to the widespread usage of nanoparticles as a therapy for cancer cell lines. Zinc oxide is biocompatible among the many materials[1-6].

The potential of ZnO NPs as chemotherapeutic and antimicrobial agents has led to a surge in interest in these NPs. ZnO NPs are highly selective for cancer cells, resulting in the generation of active oxide, hydrogen peroxide (H_2O_2) and superoxide from their surface, which may be a source of cytotoxicity in cancer cells[6-8].

The amphoteric particles that are generally used in the production of zinc oxide (ZnO), an inorganic semiconductor compound, are almost completely insoluble in water. Because of its low cost and ability to absorb UV rays between 350 and 380 nm, ZnO is widely utilised in sunscreens and other skin care products. Nanoscale ZnO particles have also been used for cellular imaging and medication administration in preclinical studies and clinical trials. For instance, it has been observed that particles with a hydrodynamic diameter of less than 100 nm achieve the highest rates of in vivo delivery. ZnO nanoparticles have been shown to have an effect on numerous cancer cells in vitro, perhaps due to the fact that Zn^{2+} stimulates the generation of reactive oxygen species (ROS). ZnO electrons can be boosted from the valence band to the conduction band by ultraviolet light, resulting in photocatalytic ROS. reported that ZnO nanoparticles administered intravenously accumulate in several tissues, particularly breast tissues, and elicit ROS-related phenomena in healthy mice, while reported that ZnO protects macrophages from the cytotoxic effects of an anticancer drug. All together, these findings suggest that ZnO may target small-cell breast cancer cells in a way that is different from how conventional chemotherapies do so. However, ZnO's efficacy against breast cancer has not been tested in live animals. Here, we put ZnO through its paces against human small-cell breast cancer cells in both culture and orthotopic mice models[9-15].

Therapeutic potential has been demonstrated in sodium alginate polymer and co-polymer pluronic F-127. Using Sodium Alginate and Pluronic F-127, the physicochemical properties of metal oxide NPs like ZnO can be modified. Researchers have begun synthesising various metal nanoparticles for use in pharmaceuticals in response to the rising demand for nanoparticles that are gentler on the environment.

Green synthesis attracts the attention of scientists since it has a small carbon footprint and is conducted with non-hazardous solvents (usually plant extracts). Leaves, fruits, rinds, barks,

seeds, and roots are mined for extracts containing reducing and stabilising agents such polyphenols, flavonoids, proteins, and sugars.

Senna auriculata Roxb. (*Cassia auriculata*, Family: Fabaceae or Leguminosae) is used to cure diabetes mellitus and rheumatism in traditional Indian medicine. This substance is used in a green synthesis to create Zno Pluronic F-127 Sodium Alginate nanoparticles.

We doped Pluronic F-127 Sodium Alginate nanoparticles (NPs) with ZnO to increase their anticancer activity and biocompatibility. The NPs were manufactured in a way that didn't endanger the natural world. Field emission scanning electron microscopy, X-ray diffraction, ultraviolet-visible spectroscopy, Fourier transform infrared spectroscopy, photoluminescence, and dynamic light scattering were all used to characterise the prepared samples. To check the Anti-cancer, anti-Fungal and anti-bacterial properties[15-21].

ZnO-infused PF 127 pluronic Sodium Alginate NPs on human breast cancer (MDA-MB-231) cells were studied. For this work, we utilised breast cancer cell lines because breast cancer is the most frequent malignancy in females and the third greatest cause of cancer death worldwide (after colorectal and lung cancer).

Division of Experiment

The Congregation of Flowers

We collected *Senna auriculata* at Trichy, not far from the airport (coordinates: 10.7204101° N, 78.7364588° E), and cleaned it twice in double-distilled water. It took 15 minutes of boiling 50-60 degree Celsius double-distilled water to extract the full flavour from 10 grams of finely chopped Flower. The extracted solution was collected in a 250 mL room temperature Erlenmeyer flask and filtered through Whatman No. 1 filter paper.

Ecological Synthesis

The production of ZnO Pluronic F-127 Sodium Alginate NPs was conducted in an environmentally responsible manner. The ZnO Pluronic F-127 Sodium Alginate NPs were made by mixing 100 mL of floral extract with 90 mL of 0.1M zinc (II) nitrate (NO3)2.6H2O After 10 minutes, the metal should have completely dissolved in the extract. Dissolving 500 mg of pluronic F-127 and 500 mg of Sodium Alginate. The concentrate yields a precipitate with a uniform colour. This solution was heated to 80 degrees Celsius and stirred constantly for 5 hours. The precipitate was then heated to 120 °C to dry it. This process yielded a nano powder of ZnO Pluronic F-127 Sodium Alginate. Five hours of annealing at 800 degrees Celsius were used to rearrange the atoms in the ZnO Pluronic F-127 Sodium Alginate NPs by increasing their vibration and diffusion inside the lattice. Any residual impurities were also removed throughout the annealing process[22-25].

Methods of Characterization

Field emission scanning electron microscopy (FESEM), X-ray diffraction (XRD), an ultraviolet-visible (UV-VIS) spectrometer, a Fourier transform infrared (FTIR) spectrometer, photoluminescence (PL), and dynamic light scattering (DLS) were used to characterise the prepared samples.

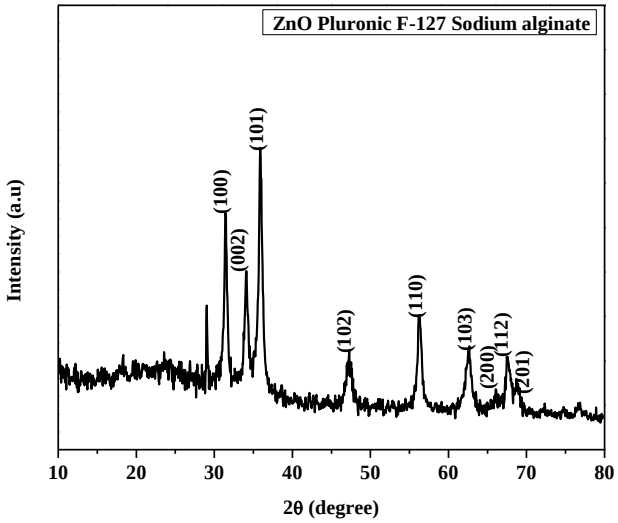

Fig 1: Shows the XRD pattern of ZnO Pluronic F-127 chitosan NPs

ZnO Pluronic F-127 Sodium Alginate NPs X-ray diffraction patterns are displayed in Figure 1. The diffraction angle 2θ peaks observed at 31.44°, 34.08°, 35.85°, 47.16°, 56.20°, 62.60°, 67.53° and 68.89° which corresponds to the hkl plans (100), (002), (101), (102), (110), (103), (200), (112), (201), (004) respectively, and those results are perfectly matched with (JCPDS NP: 36-1451) for wurtzite hexagonal structure . No impurity peaks were seen in ZnO Pluronic F-127 Sodium Alginate NPs, but there was a slight shift in the lower 2θ values compared to the ZnO NPs (Fig. 1). The Debye-Scherrer relation n was determined by using the crystallite size $D = \frac{0.9\,\lambda}{\beta cos\,\theta}$ is the typical size of a crystal. ZnO Pluronic F-127 Sodium Alginate NPs have an average crystalline size of 22.52 nm[27-30].

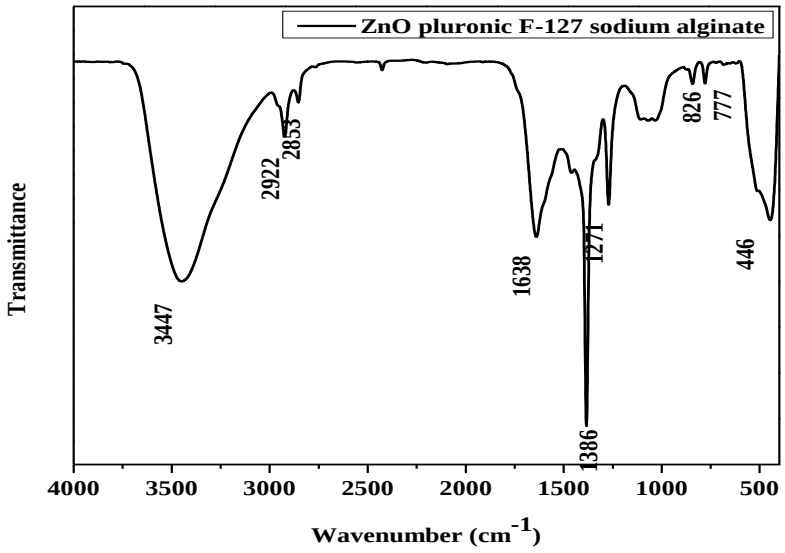

Figure 2: Shows the FTIR spectrum of ZnO Pluronic F-127 Sodium Alginate NPs

Hydroxyl O-H stretching vibrations in ZnO NPs are observed at 3447 cm^{-1}. Sodium alginate has these notable peaks in its spectrum: The -CH(CH2) group caused the asymmetric and symmetric peaks to appear at 2922 $cm^{-1}$and 2854 cm^{-1}, respectively.Plant leaf capping on ZnO samples is caused by the C=C stretching group at 1638 cm^{-1}. The peak Plunoric F-127 molecule has a C=O symmetric stretching vibration at 1386 cm^{-1}, a C-O stretching vibration at 1271 cm^{-1}, and a C=H bending vibration at 826 cm^{-1}. ZnO Pluronic F-127 Sodium Alginate NPs have a Zn-O stretching band at 446 cm^{-1}. This FTIR demonstrates the plant, ZnO, Sodium Alginate, and Plunoric F-127 are all present[30-35].

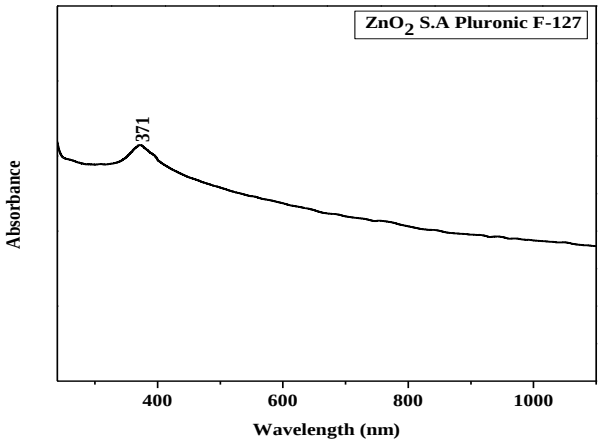

Fig3: UV-visible absorption by ZnO Pluronic F-127 Sodium Alginate nanoparticles

ZnO Pluronic F-127 Sodium Alginate nanoparticles' UV-visible absorption spectrum is shown in the figure. The ultraviolet ranged in size from 190 to 1100 nanometers. ZnO Pluronic F-127 Sodium Alginate NPs can be evaluated with the help of a UV-Vis spectrophotometer because their optical properties are directly related to their size. When the size of ZnO Pluronic F-127 Sodium Alginate nanoparticles (NPs) is changed, the position of the absorption band or the surface Plasmon resonance band moves. As the particle size decreases, the absorption edge is expected to move to a higher energy due to the quantum confinement effect[36-40]. The results of this new study lend further credence to those of the earlier studies. ZnO Pluronic F-127 Sodium Alginate nanoparticles have a maximum absorption at 371 nm.

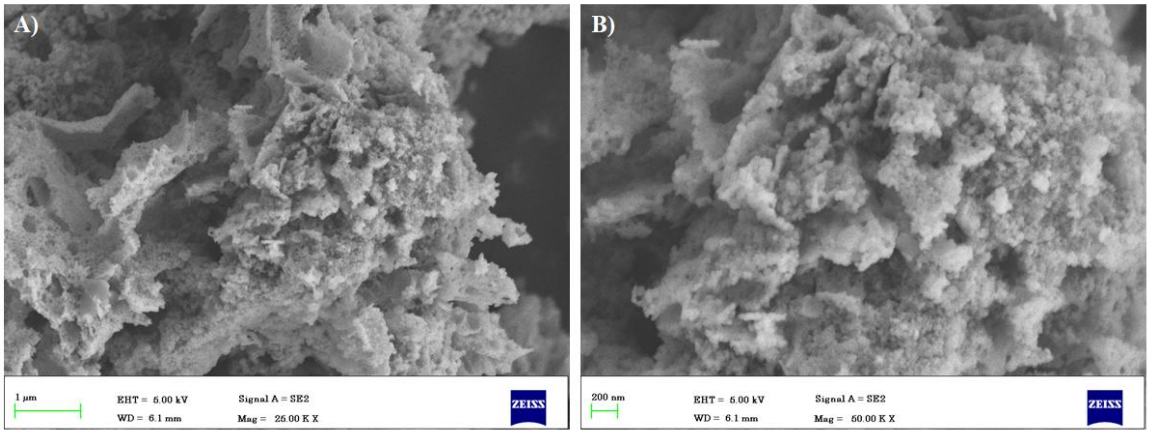

Fig 4 (A-B) Shows the Scanning electron microscopy (SEM) Images of ZnO Pluronic F-127 Sodium Alginate

Scanning electron microscopy (SEM) was used to look at the ZnO Pluronic F127 Sodium Alginate morphologies. The tetrahedral particles that make up ZnO have a diameter of 10-20 nm, as seen in the low-magnification SEM image in Figure 5 (A). High-magnification SEM images of ZnO Pluronic F127 Sodium Alginate were analysed to better comprehend its structural characteristics (Fig.4(B)). Nanoparticles from several nanometers down to one nanometer in size coat the surface of ZnO Pluronic F127 Sodium Alginate particles. In addition, some tiny, elongated microspheres could be made out in the gaps between the larger particles[41-45]. Zno nanoparticle assembly could be influenced by Sodium Alginate and Pluronic F-127.

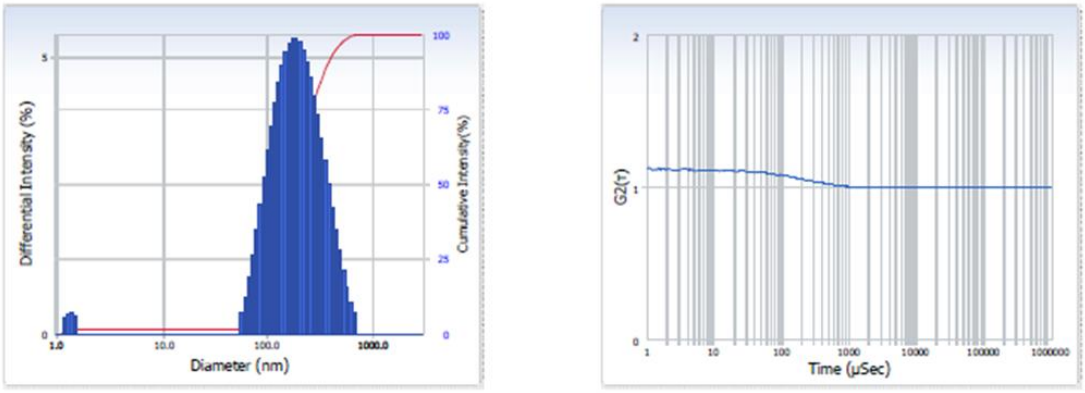

Fig 6 (DLS) dynamic light scattering of Zno Pluronic F-127 Chiosan NPs

Particle shipping dimensions in aqueous solutions were calculated using dynamic light scattering (DLS). ZnO Pluronic F-127 Sodium Alginate NPs increased in size to 181 nm (nanoparticle itself, surrounded by water molecules) as measured by DLS. This happened because the hydrodynamic size of the ZnO Pluronic F-127 Sodium Alginate NPs was determined by the molecules of the liquid surrounding them. The growth and nucleation rate of the ZnO NPs were slowed down by the presence of exogenous substances like Pluronic F-127 and Sodium Alginate, resulting in smaller particle size[46-48].

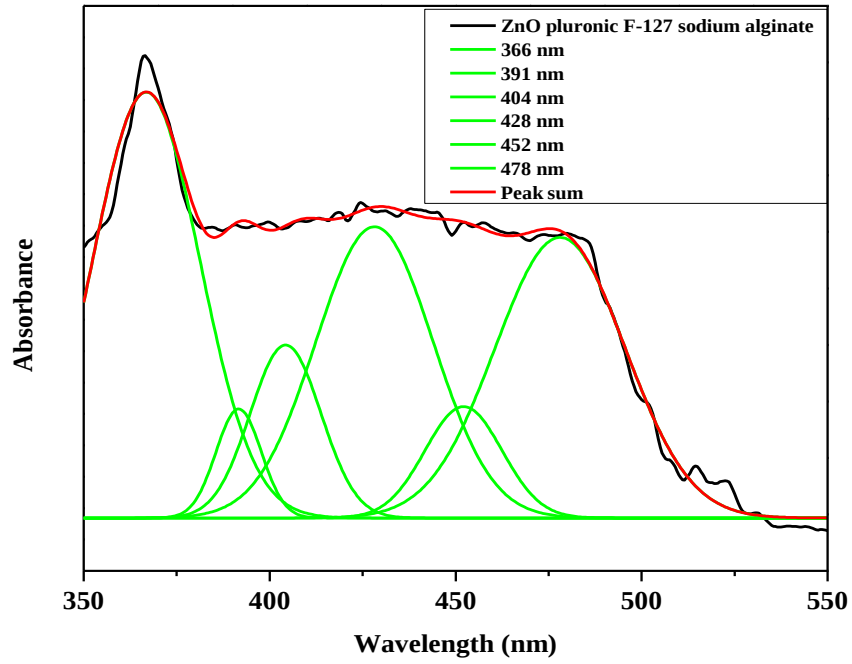

Fig 4: photoluminescence spectra of the Zno Pluronic F-127 Sodium Alginate

The photoluminescence spectra of ZnO Pluronic F-127 Sodium Alginate NPs are shown here ,Excited at a wavelength of 325 nm, Each nanoparticle has very similar optical properties across the board, with peaks in their spectra located very close to one another. By contrasting the spectra, we can see this. This is evident from the fact that the top spots are relatively equal to one another. ZnO Pluronic F-127 Sodium Alginate NPs had emission peaks at 366,391,404,428,452, and 478 nm, as measured by spectroscopy. ZnO Pluronic F-127 Sodium Alginate NPs have a violet emission centre at 478 nm because an electron has jumped from a shallow donor level of natural Zn interstitials to the top level of the valence band. When an electron leaves a naturally occurring Zn interstitial, this transition takes place. This change occurs when an electron travels all the way from a lower donor level to the top level. When the light is analysed, this shift occurs at a wavelength of 404 nm. As the electron recedes from a naturally occurring Zn interstitial, this change takes place[49-51]. ZnO

Pluronic F-127 Sodium Alginate NPs have blue emission peaks at 452 and 478 nm, respectively.

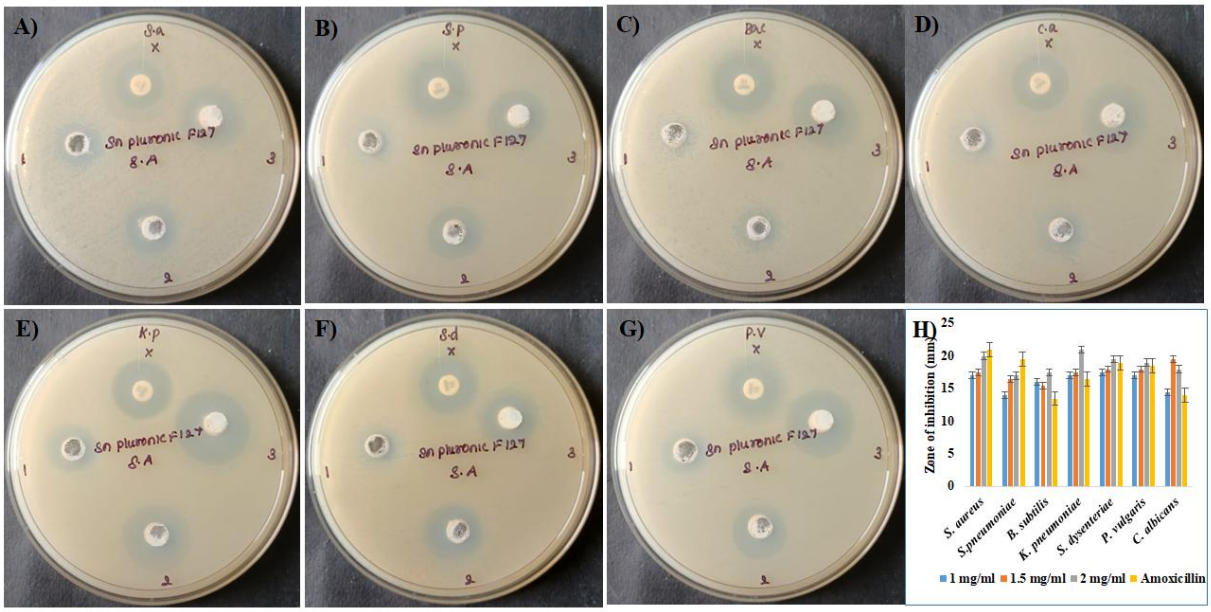

FIG:7 Antibacterial and Anti-fungal zone of inhibition (A-G) and Graph of Antibacterial and Antifungal Activity (H) for the prepared Zno Pluronic F-127 Sodium Alginate

Through the well-diffusion method, various types of *S. aureus*, *K. pneumoniae*, *S. dysenteriae*, *B. cereus*, and *P. valgaris* have been investigated to find out their level of susceptibility to amoxicillin and Zno Pluronic F-127 Sodium Alginate NPs. Gram-positive bacterial cultures typically display a higher level of activity when compared to their Gram-negative counterparts. Gram-positive cultures generate significantly more activity than gram-negative cultures do due to the fact that the cell walls of gram-positive bacteria are completely different from those of gram-negative bacteria. Because their cell walls are composed of multiple layers of peptidoglycan, Gram-positive bacteria are able to withstand a variety of conditions and are resistant to infection. In the same way that surface proteins can

be anchored to the peptidoglycan, polymers such as teichoic and lipoteichoic acids can also be anchored to the peptidoglycan. Porins, a thin layer of peptidoglycan, and lipopolysaccharide (also known as LPS) are the three components that make up the outer membrane of Gram-negative bacteria. This outer membrane also contains the LPS that was previously mentioned. ZnO has difficulty killing Gram-negative bacteria because these bacteria have an outer membrane to protect themselves. Because of this, we have reason to believe that the success of ZnO NP against Gram-negative bacteria can be attributed to this subset. According to the findings of the XRD analysis, the ZnO Pluronic F-127 Sodium Alginate sample contained NPs with an average size of 22.52 nanometers. There is a possibility that nanoparticles become more toxic as their size decreases. This is due to the fact that a greater quantity of ZnO particles are required to completely cover the surface of the bacteria, which in turn results in a greater quantity of reactive oxygen species (ROS). The antibacterial activity of ZnO NPs may be proportional to the particle size[52-60]. This is due to the fact that smaller NPs are able to penetrate deeper into bacteria than larger ones . This is because the larger NP has a greater interfacial area than the smaller NP does, which is the reason for this result.

The well diffusion method is used to investigate whether or not the biologically synthesised ZnO Pluronic F-127 Sodium Alginate is effective in inhibiting the development of bacteria and fungi. An overgrowth of *Candida albicans* may be successfully treated with sodium alginate that has been produced with ZnO Pluronic F-127. The size of the inhibition zone that was calculated demonstrates that when compared to ZnO NPs, the doped nanomaterial ZnO Pluronic F-127 Chitosan is more effective at inhibiting the growth of fungi. It's possible that the antifungal properties of *Senna auriculata* can boost the efficiency of naturally occurring ZnO Pluronic F-127 Sodium Alginate.

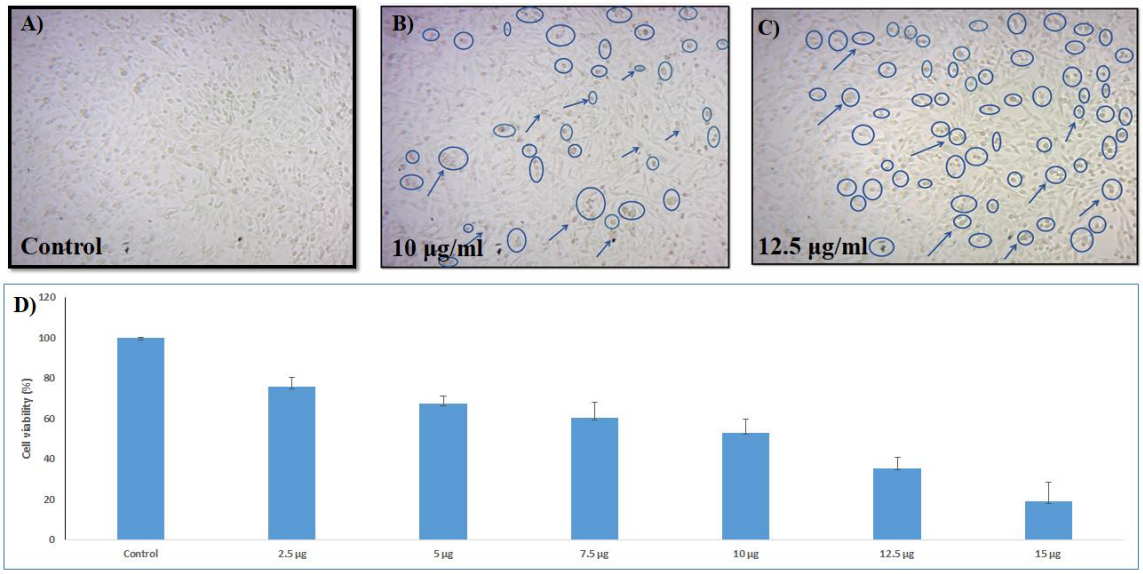

Fig 8: Morphological changes in control (A) and ZnO Pluronic F-127 Sodium Alginate (B-C) treated Breast cancer (MDA-MB-231) cells for 24 h. (D) Graphical presentation of Control and treated cells.

ZnO Pluronic F-127 Sodium Alginate's anticancer efficacy was shown in Fig. 8. By conducting research with the human breast cancer cell line MDA-MB-237. ZnO Pluronic F-127 Sodium Alginate NPs' IC_{50} value for cytotoxicity was determined to be 10 g/ml after incubation for 24 hours at concentrations ranging from 0 to 15 g/ml. ZnO Pluronic F-127 Sodium Alginate NPs cytotoxicity IC_{50} was calculated to arrive at this value.

The cytotoxicity of Nanomaterials can be affected by their size, solubility, surface defects (oxygen vacancies), and the production of reactive oxygen species (ROS). This study concludes that oxygen vacancies (Ov) in ZnO Pluronic F-127 sodium alginate NPs are responsible for the blue emission peak observed in the PL spectrum. This maximum is located between the wavelengths of 470 nm. This is due to the high concentration of free radicals and reactive oxygen species (ROS). High levels of oxidative stress, caused by

reactive oxygen species (ROS, OH, H_2O_2, andO_2) and their interactions with macromolecules (DNA, lipids, and proteins), were observed in cancer cells[61-66].

Conclusion

For the purpose of determining the cytotoxicity of ZnO Pluronic F-127 Sodium Alginate NPs, the present study made use of cancer-causing cells in addition to a wide variety of bacteria, both gram-negative and gram-positive bacteria included. In order to make the ZnO Pluronic F-127 Sodium Alginate NPs, leaf extracts from the *Senna auriculata* plant were put through a process known as green precipitation. This procedure resulted in the creation of the NPs. Using X-ray diffraction, the researchers found that ZnO Pluronic F-127 Sodium Alginate NPs with a wurtzite hexagonal structure have an average size of 17 nm. Using scanning electron microscopy, researchers were able to determine that ZnO Pluronic F-127 Sodium Alginate NPs are composed of particles with a tetrahedral shape that range in size from 10 to 20 nanometers. Pluronic F-127 and Sodium Alginate form with ZnO NPs at the same time, as shown by FTIR spectra; this indicates the formation of powerful higher intermolecular hydrogen bonds in the material matrix. In accordance with the findings of the PL analysis, the band emission of the ZnO Pluronic F-127 Sodium Alginate NPs was determined to be caused by zinc vacancies, oxygen vacuoles, and surface flaws. In the laboratory, it was discovered that ZnO Pluronic F127 Sodium Alginate NPs were more effective at killing bacteria than the antibiotic amoxicillin, which is typically prescribed to patients. The human breast cancer cell line was resistant to the cytotoxic effects of the compound despite the fact that ZnO Pluronic F-127 Sodium Alginate NPs were effective against other types of cancer cell lines. ZnO Pluronic F-127 Sodium Alginate NPs, which was synthesised, was effective against the test bacteria as well as the cancer cell lines. It was discovered that Sodium Alginate nanoparticles have powerful antibacterial and anticancer effects. In most cases, the evidence points to the synthesis as being the factor that caused these effects.

Author Contributions:

Mr.GSK carried out the preparation of the nanoparticles and executes the physical characterization studies and contributed to the main text of the manuscript. Dr.AS checked the scientific information and flow of the text to maintain a better readability. Further this research work is not funded by any agency.

Compliance with ethical standards:

Conflict of interest: The author declared that they have no conflict of interest

Reference:

1. Parkin DM, Whelan SL and Ferlay J. et al. 2002. IARC Scientific Publications, 155.
2. E. R. Arakelova, S. G. Grigoryan, F. G. Arsenyan, N. S. Babayan, R. M. Grigoryan, N. K. Sarkisyan. 2014. Intl. J. Biomed. Pharma. Sci., Vol. 8, No. 1.
3. Ameer Azam, Faheem Ahmed. et al. 2009. Int. J. Th. and App. Sci, Vol. 1, No. 2, pp. 12-14.
4. Liming Shen and Ningzhong Bao. et al. 2006. Nanotechnology, Vol. 17, pp. 5117–5123.
5. Mosmann T. 1983. J. Immunol. Methods, Vol. 65, 55-63. Smalley KS, Herlyn M. Towards the targeted therapy of melanoma. Mini Rev Med Chem. 2006;6(4):387-93.
6. Vidhya, E., S. Vijayakumar, S. Prathipkumar, and P. K. Praseetha. "Green way biosynthesis: Characterization, antimicrobial and anticancer activity of ZnO nanoparticles." *Gene Reports* 20 (2020): 100688.
7. Langer R. Drug delivery and targeting. Nature. 1998;392(6679 Suppl):5-10.
8. Gowda R, Jones NR, Banerjee S, Robertson GP. Use of Nanotechnology to Develop Multi-Drug Inhibi- tors For Cancer Therapy. J Nanomed Nanotechnol. 2013;4(6).
9. Wang R, Billone PS, Mullett WM. Nanomedicine in Action: An Overview of Cancer Nanomedicine on the Market and in Clinical Trials. Journal of Nano- materials. 2013;2013:12.
10. McNeil SE. Nanoparticle therapeutics: a personal perspective. Wiley Interdiscip Rev Nanomed Nanobiotechnol. 2009;1(3):264-71.

11. Vizirianakis IS. Nanomedicine and personalized medicine toward the application of pharmacotyp- ing in clinical practice to improve drug-delivery outcomes. Nanomedicine: Nanotechnology, Biology and Medicine. 2011;7(1):11-7.
12. Godin B, Sakamoto JH, Serda RE, Grattoni A, Bouamrani A, Ferrari M. Emerging Applications of Nanomedicine for Therapy and Diagnosis of Cardiovascular Diseases. Trends Pharmacol Sci. 2010;31(5):199-205.
13. Bhattacharyya S, Kudgus R, Bhattacharya R, Mukherjee P. Inorganic Nanoparticles in Cancer Therapy. Pharmaceutical Research. 2011;28(2): 237-59.
14. Vinardell M, Mitjans M. Antitumor Activities of Metal Oxide Nanoparticles. Nanomaterials. 2015;5(2):1004.
15. Orel V, Shevchenko A, Romanov A, Tselepi M, Mitrelias T, Barnes CH, et al. Magnetic properties and antitumor effect of nanocomplexes of iron oxide and doxorubicin. Nanomedicine. 2015;11(1): 47-55.
16. Zhang AP, Sun YP. Photocatalytic killing effect of TiO2 nanoparticles on Ls-174-t human colon carcinoma cells. World J Gastroenterol. 2004;10(21): 3191-3.
17. Thevenot P, Cho J, Wavhal D, Timmons RB, Tang L. Surface chemistry influences cancer killing effect of TiO2 nanoparticles. Nanomedicine. 2008;4(3): 226-36.
18. Wason MS, Colon J, Das S, Seal S, Turkson J, Zhao J, et al. Sensitization of pancreatic cancer cells to radiation by cerium oxide nanoparticle-induced ROS production. Nanomedicine. 2013;9(4):558-69.
19. Shen C, James SA, de Jonge MD, Turney TW, Wright PF, Feltis BN. Relating cytotoxicity, zinc ions, and reactive oxygen in ZnO nanoparticle-exposed human immune cells. Toxicol Sci. 2013;136(1): 120-30.
20. Sankar R, Maheswari R, Karthik S, Shivashangari KS, Ravikumar V. Anticancer activity of Ficus religiosa engineered copper oxide nanoparticles. Mater Sci Eng C Mater Biol Appl. 2014;44:234-9.
21. Sivaraj R, Rahman PK, Rajiv P, Narendhran S, Venckatesh R. Biosynthesis and characterization of Acalypha indica mediated copper oxide nanoparti- cles and evaluation of its antimicrobial and anti- cancer activity. Spectrochim Acta A Mol Biomol Spectrosc. 2014;129:255-8.
22. Narayanan KB, Sakthivel N. Biological synthesis of metal nanoparticles by microbes. Adv Colloid Interface Sci. 2010;156(1-2):1-13.

23. Meng H, Wang M, Liu H, Liu X, Situ A, Wu B, et al. Use of a lipid-coated mesoporous silica nanoparti- cle platform for synergistic gemcitabine and paclitaxel delivery to human pancreatic cancer in mice. ACS Nano. 2015;9(4):3540-57.
24. Greco RS, Prinz FB, Smith RL. Nanoscale technolo- gy in biological systems. Boca Raton: CRC Press; 2005.
25. Kołodziejczak-Radzimska A, Jesionowski T. Zinc Oxide—From Synthesis to Application: A Review. Materials. 2014;7(4):2833.
26. Nel A, Xia T, Madler L, Li N. Toxic potential of materials at the nanolevel. Science. 2006;311(5761): 622-7.
27. Vaseem M, Umar A, Hahn Y-B. ZnO nanoparticles: growth, properties, and applications. Metal Oxide Nanostructures and Their Applications, Chapter 4, Publisher: American Scientific Publishers, New York; 2010. p. 1-36.
28. Zhou J, Xu NS, Wang ZL. Dissolving behavior and stability of ZnO wires in biofluids: a study on biodegradability and biocompatibility of ZnO nanostructures. Advanced Materials-Deerfield Beach then Weinheim. 2006;18(18):2432.
29. Hanley C, Layne J, Punnoose A, Reddy KM, Coombs I, Coombs A, et al. Preferential killing of cancer cells and activated human T cells using ZnO nanoparticles. Nanotechnology. 2008;19(29): 295103.
30. Huang K, Ma H, Liu J, Huo S, Kumar A, Wei T, et al. Size-dependent localization and penetration of ultrasmall gold nanoparticles in cancer cells, multicellular spheroids, and tumors in vivo. ACS Nano. 2012;6(5):4483-93.
31. Rasmussen JW, Martinez E, Louka P, Wingett DG. Zinc oxide nanoparticles for selective destruction of tumor cells and potential for drug delivery applica- tions. Expert Opin Drug Deliv. 2010;7(9):1063-77.
32. Davis ME, Chen ZG, Shin DM. Nanoparticle therapeutics: an emerging treatment modality for cancer. Nat Rev Drug Discov. 2008;7(9):771-82.
33. King J, Turnlund J. Human Zinc Requirements. In: Mills C, editor. Zinc in Human Biology. ILSI Human Nutrition Reviews: Springer London; 1989. p. 335-50.
34. Chapter 16. Zinc: agriculture and consumer protec- tion; 2015 (cited 4 October 2015). Available from: http://www.fao.org/docrep/004/y2809e/ y2809e0m.htm#bm22.
35. Ho E. Zinc deficiency, DNA damage and cancer risk. J Nutr Biochem. 2004;15(10):572-8.
36. Ng KW, Khoo SP, Heng BC, Setyawati MI, Tan EC, Zhao X, et al. The role of the tumor suppressor p53 pathway in the cellular DNA damage response to zinc oxide nanoparticles. Biomaterials. 2011;32(32): 8218-25.

37. Cho Y, Gorina S, Jeffrey P, Pavletich N. Crystal structure of a p53 tumor suppressor-DNA complex: understanding tumorigenic mutations. Science. 1994;265(5170):346-55.
38. Dhawan DK, Chadha VD. Zinc: a promising agent in dietary chemoprevention of cancer. Indian J Med Res. 2010;132:676-82.
39. Beyersmann D. Homeostasis and Cellular Func- tions of Zinc. Materialwissenschaft und Werkstoff- technik. 2002;33(12):764-9.
40. Ho E, Ames BN. Low intracellular zinc induces oxidative DNA damage, disrupts p53, NFkappa B, and AP1 DNA binding, and affects DNA repair in a rat glioma cell line. Proc Natl Acad Sci USA. 2002;99(26):16770-5.
41. Zowczak M, Iskra M, Torlinski L, Cofta S. Analysis of serum copper and zinc concentrations in cancer patients. Biol Trace Elem Res. 2001;82(1-3):1-8.
42. Abnet CC, Lai B, Qiao YL, Vogt S, Luo XM, Taylor PR, et al. Zinc concentration in esophageal biopsy specimens measured by x-ray fluorescence and esophageal cancer risk. J Natl Cancer Inst. 2005;97(4):301-6.
43. Costello LC, Franklin RB, Feng P, Tan M, Bagasra O. Zinc and prostate cancer: a critical scientific, medical, and public interest issue (United States). Cancer Causes Control. 2005;16(8):901-15.
44. Nel AE, Madler L, Velegol D, Xia T, Hoek EM, Somasundaran P, et al. Understanding biophysico- chemical interactions at the nano-bio interface. Nat Mater. 2009;8(7):543-57.
45. Min Y, Akbulut M, Kristiansen K, Golan Y, Israel- achvili J. The role of interparticle and external forces in nanoparticle assembly. Nat Mater. 2008;7(7): 527-38.
46. Kim HY, Sofo JO, Velegol D, Cole MW, Lucas AA. Van der Waals dispersion forces between dielectric nanoclusters. Langmuir. 2007;23(4):1735-40.
47. Geiser M, Rothen-Rutishauser B, Kapp N, Schurch S, Kreyling W, Schulz H, et al. Ultrafine particles cross cellular membranes by nonphagocytic mechanisms in lungs and in cultured cells. Environ Health Perspect. 2005;113(11):1555-60.
48. Rimai DS, Quesnel DJ, Busnaina AA. The adhesion of dry particles in the nanometer to micrometer-size range. Colloids and Surfaces A: Physicochemical and Engineering Aspects. 2000;165(1–3):3-10.
49. Buzea C, Pacheco I, Robbie K. Nanomaterials and nanoparticles: Sources and toxicity. Biointerphases. 2007;2(4):MR17-MR71(page 55)
50. Peters A, Veronesi B, Calderón-Garcidueñas L, Gehr P, Chen LC, Geiser M, et al. Translocation and potential neurological effects of fine and ultrafine particles: a critical update. Particle and Fibre Toxicology. 2006;3:13.

51. Garcia-Garcia E, Andrieux K, Gil S, Kim HR, Le Doan T, Desmaele D, et al. A methodology to study intracellular distribution of nanoparticles in brain endothelial cells. Int J Pharm. 2005;298(2):310-4.
52. Lundqvist M, Stigler J, Elia G, Lynch I, Cedervall T, Dawson KA. Nanoparticle size and surface proper- ties determine the protein corona with possible implications for biological impacts. Proc Natl Acad Sci USA. 2008;105(38):14265-70.
53. Cedervall T, Lynch I, Lindman S, Berggard T, Thulin E, Nilsson H, et al. Understanding the nanoparticle-protein corona using methods to quantify exchange rates and affinities of proteins for nanoparticles. Proc Natl Acad Sci USA. 2007;104(7): 2050-5.
54. Verderio P, Avvakumova S, Alessio G, Bellini M, Colombo M, Galbiati E, et al. Delivering Colloidal Nanoparticles to Mammalian Cells: A Nano–Bio Interface Perspective. Advanced Healthcare Materials. 2014;3(7):957-76.
55. Xia T, Kovochich M, Brant J, Hotze M, Sempf J, Oberley T, et al. Comparison of the abilities of ambient and manufactured nanoparticles to induce cellular toxicity according to an oxidative stress paradigm. Nano Lett. 2006;6(8):1794-807.
56. Turney TW, Duriska MB, Jayaratne V, Elbaz A, O'Keefe SJ, Hastings AS, et al. Formation of zinccontaining nanoparticles from Zn(2)(+) ions in cell culture media: implications for the nanotoxicology of ZnO. Chem Res Toxicol. 2012;25(10):2057-66.
57. Chasapis CT, Loutsidou AC, Spiliopoulou CA, Stefanidou ME. Zinc and human health: an update. Arch Toxicol. 2012;86(4):521-34.
58. Casey JR, Grinstein S, Orlowski J. Sensors and regulators of intracellular pH. Nat Rev Mol Cell Biol. 2010;11(1):50-61.
59. Song W, Zhang J, Guo J, Zhang J, Ding F, Li L, et al. Role of the dissolved zinc ion and reactive oxygen species in cytotoxicity of ZnO nanoparticles. Toxicol Lett. 2010;199(3):389-97.
60. Manke A, Wang L, Rojanasakul Y. Mechanisms of Nanoparticle-Induced Oxidative Stress and Toxici- ty. BioMed Research International. 2013;2013:15.
61. Driscoll K, Howard B, Carter J, Janssen YW, Mossman B, Isfort R. Mitochondrial-Derived Oxidants and Quartz Activation of Chemokine Gene Expression. In: Dansette P, Snyder R, Dela- forge M, Gibson GG, Greim H, Jollow D, et al., editors. Biological Reactive Intermediates VI. Advances in Experimental Medicine and Biology. 500: Springer US; 2001. p. 489-96.

62. Wilson MR, Lightbody JH, Donaldson K, Sales J, Stone V. Interactions between Ultrafine Particles and Transition Metals in Vivo and in Vitro. Toxi- cology and Applied Pharmacology. 2002;184(3): 172-9.
63. Gyu-Chul Y, Chunrui W, Won Il P. ZnO nanorods: synthesis, characterization and applications. Semiconductor Science and Technology. 2005;20(4):S22.
64. Kim Y-J, Yu M, Park H-O, Yang S. Comparative study of cytotoxicity, oxidative stress and genotox- icity induced by silica nanomaterials in human neuronal cell line. Molecular & Cellular Toxicology. 2010;6(4):336-43.
65. Valko M, Rhodes CJ, Moncol J, Izakovic M, Mazur M. Free radicals, metals and antioxidants in oxida- tive stress-induced cancer. Chem Biol Interact. 2006;160(1):1-40.
66. Kawanishi S, Hiraku Y, Murata M, Oikawa S. The role of metals in site-specific DNA damage with reference to carcinogenesis1,2. Free Radical Biology and Medicine. 2002;32(9):822-32.